Journal of the American College of Cardiology
© 2008 by the American College of Cardiology Foundation
Published by Elsevier Inc.

Vol. 52, No. 16, 2008
ISSN 0735-1097/08/$34.00
doi:10.1016/j.jacc.2008.07.013

A Novel *SCN5A* Gain-of-Function Mutation M1875T Associated With Familial Atrial Fibrillation

Takeru Makiyama, MD, PHD,* Masaharu Akao, MD, PHD,* Satoshi Shizuta, MD,* Takahiro Doi, MD,* Kei Nishiyama, MD,* Yuko Oka, MD,† Seiko Ohno, MD, PHD,* Yukiko Nishio, MD,* Keiko Tsuji, MS,† Hideki Itoh, MD, PHD,† Takeshi Kimura, MD, PHD,* Toru Kita, MD, PHD,* Minoru Horie, MD, PHD†

Kyoto and Otsu, Japan

Objectives This study describes a novel heterozygous gain-of-function mutation in the cardiac sodium (Na^+) channel gene, *SCN5A*, identified in a Japanese family with lone atrial fibrillation (AF).

Background *SCN5A* mutations have been associated with a variety of inherited arrhythmias, but the gain-of-function type modulation in *SCN5A* is associated with only 1 phenotype, long-QT syndrome type 3 (LQTS3).

Methods We studied a Japanese family with autosomal dominant hereditary AF, multiple members of which showed an onset of AF or frequent premature atrial contractions at a young age.

Results The 31-year-old proband received radiofrequency catheter ablation, during which time numerous ectopic firings and increased excitability throughout the right atrium were documented. Mutational analysis identified a novel missense mutation, M1875T, in *SCN5A*. Further investigations revealed the familial aggregation of this mutation in all of the affected individuals. Functional assays of the M1875T Na^+ channels using a whole-cell patch-clamp demonstrated a distinct gain-of-function type modulation; a pronounced depolarized shift (+16.4 mV) in $V_{1/2}$ of the voltage dependence of steady-state inactivation; and no persistent Na^+ current, which is a defining mechanism of LQTS3. These biophysical features of the mutant channels are potentially associated with increased atrial excitability and normal QT interval in all of the affected individuals.

Conclusions We identified a novel *SCN5A* mutation associated with familial AF. The mutant channels displayed a gain-of-function type modulation of cardiac Na^+ channels, which is a novel mechanism predisposing to increased atrial excitability and familial AF. This is a new phenotype resulting from the *SCN5A* gain-of-function mutations and is distinct from LQTS3. (J Am Coll Cardiol 2008;52:1326–34) © 2008 by the American College of Cardiology Foundation

The cardiac sodium (Na^+) channel plays a crucial role in cardiac excitation/contraction via initiating the action potential of the conduction system and working myocytes. Mutations in *SCN5A*—which encodes the α-subunit of voltage-gated cardiac Na^+ channels—have been associated with a variety of cardiac arrhythmias. The loss-of-function mutations result in Brugada syndrome (1), idiopathic ventricular fibrillation (2), cardiac conduction disease (3), or congenital sick sinus syndrome (4), whereas the gain-of-function type modulation in *SCN5A* is associated with only 1 phenotype, long-QT syndrome type 3 (LQTS3) (5).

We reported on the screening for *SCN5A* mutations in Japanese patients with Brugada syndrome (6) and now have extended the cohort to various inherited arrhythmias, given the wide spectrum of clinical phenotypes of cardiac Na^+ channelopathies. In the present study, in a Japanese family with lone atrial fibrillation (AF), we identified a novel missense mutation of *SCN5A* (M1875T). Until recently, only potassium channel mutations have been linked to familial AF (7–10); however, 3 recent reports have identified *SCN5A* loss-of-function mutations: D1275N in 2 families with atrial arrhythmias (AF, cardiac conduction disease, or sick sinus syndrome) plus dilated cardiomyopathy (11,12), and N1986K in a family with lone AF (13). Thus, this is the first report to identify an *SCN5A* gain-of-function type mutation in familial AF.

From the *Department of Cardiovascular Medicine, Kyoto University Graduate School of Medicine, Kyoto, Japan; and the †Department of Cardiovascular and Respiratory Medicine, Shiga University of Medical Science, Otsu, Japan. This work was supported by research grants from the Japan Heart Foundation/Pfizer Japan Inc. Grant for Research on Cardiovascular Disease; Grants-in-Aid in Scientific Research from the Ministry of Education, Culture, Science, and Technology of Japan; and a Health Sciences Research Grant (H18-Research on human Genome-002) from the Ministry of Health, Labor and Welfare of Japan.

Manuscript received March 3, 2008; revised manuscript received July 7, 2008, accepted July 10, 2008.

Methods

Clinical evaluation. This study was approved by the Institutional Ethics Committee, and all patients provided informed consent. Affected individuals were considered as having AF or premature atrial contractions (PACs) when documented by 12-lead electrocardiograms (ECGs). Lone AF was defined as onset of AF at age <65 years without structural heart disease, hypertension, hyperthyroidism, myocardial infarction, or congestive heart failure. Paroxysmal AF was defined as sporadic AF lasting >30 s for <7 days. When sustained beyond 7 days, AF was considered persistent. Atrial fibrillation refractory to cardioversion or not attempted was classified as permanent. In both sinus rhythm and AF, the mean QT and RR intervals were measured from 3 and 6 consecutive beats, respectively.

Deoxyribonucleic acid (DNA) isolation and mutation analysis. Genomic DNA was isolated from blood lymphocytes and screened for candidate genes by denaturing high-performance liquid chromatography with a WAVE System Model 3500 (Transgenomic, Omaha, Nebraska). Abnormal conformers were amplified by polymerase chain reaction, and sequencing was performed on an ABI PRISM 3100 DNA sequencer (Applied Biosystems, Foster City, California).

Site-directed mutagenesis and electrophysiology. To construct the *SCN5A* mutant, we adopted site-directed mutagenesis performed via a kit, QuickChange II XL (Stratagene, La Jolla, California). The human cell line HEK293 cultured in a 35-mm dish was transiently transfected with 0.5 μg of either pRcCMV-WT or mutant complementary DNA in combination with 0.5 μg of the bicistronic plasmid (pEGFP-IRES-hβ1) encoding enhanced green fluorescent protein and the human β1-subunit (hβ1). The Na^+ currents were recorded 48 h after transfection with the whole-cell patch-clamp technique at 22°C to 23°C as described elsewhere (14). Results are expressed as mean ± SEM, and statistical significance was established with the Student *t* test. Statistical significance was assumed for $p < 0.05$.

Abbreviations and Acronyms

- **AF** = atrial fibrillation
- **AT** = atrial tachycardia
- **ECG** = electrocardiogram
- **LQTS3** = long-QT syndrome type 3
- **PAC** = premature atrial contraction
- **WT** = wild-type

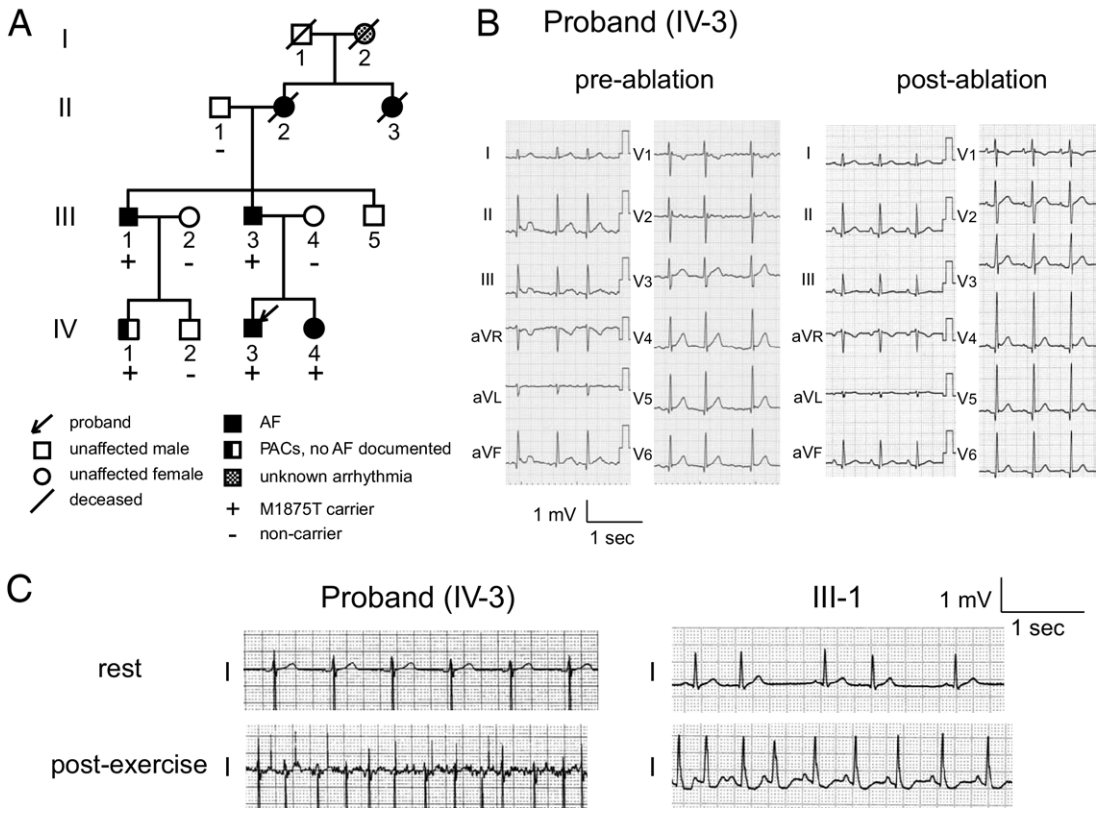

Figure 1 Pedigree and Clinical Features

(A) Pedigree of the family. Phenotypic traits are designated within pedigree symbols. **(B)** Electrocardiograms (ECGs) obtained from the proband, IV-3, before (**left panel**, atrial fibrillation [AF]) and after (**right panel**, sinus rhythm) he underwent radiofrequency catheter ablation. **(C)** At rest and post-exercise ECGs recorded from the proband (IV-3) and his uncle (III-1). Exercise-induced AF for the proband and atrial tachycardia for the uncle can be observed. *Continued on next page.*

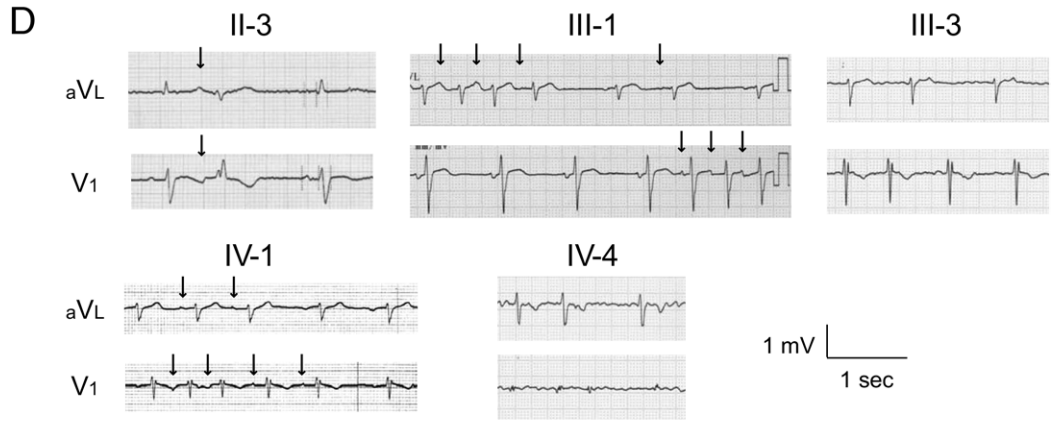

Figure 1 Continued

(D) Electrocardiograms recorded from other affected individuals. **Arrows** indicate P waves of premature atrial contractions (PACs) in II-3, III-1, and IV-1. III-3 and IV-4 demonstrated AF.

Results

Clinical features. We studied a Japanese family with autosomal dominant hereditary AF that spanned 3 generations (Fig. 1A). The proband (IV-3) (Fig. 1A), a 31-year-old man, first experienced repetitive palpitation due to frequent PACs at age 18, which later progressed to paroxysmal AF and atrial tachycardia (AT) at age 27 years (pre-ablation) (Fig. 1B).

Six family members, along with the proband, presented with either AF or frequent PACs (Fig. 1A). The majority shared a similar clinical course with the proband—palpitations due to PACs start in their teens, which later progress to paroxysmal and ultimately persistent AF (Table 1). The proband and his uncle (III-1) showed exercise-induced AT and/or AF (Fig. 1C). The proband's cousin (IV-1) presented with frequent PACs (Fig. 1D) that have not yet progressed to AF. The ECGs of the affected relatives—with the exception to the proband's aunt (II-3), who received disopyramide—did not show any QT prolongation (Fig. 1D, Table 1). Interestingly, the analysis of P wave morphology in the affected family members revealed that the majority of PAC foci were localized in the right atrium (Fig. 1D). The affected individuals received various antiarrhythmic agents (Table 1) but, in most cases, to no avail. There was neither structural heart disease nor a history of major ventricular arrhythmias or sudden cardiac death in this family.

At age 27 years, the proband underwent radiofrequency catheter ablation. Intravenous administration of isoproterenol induced repetitive ATs from multiple origins in the right atrium (Fig. 2A). We successfully ablated the major origin, located in the lower-right atrial septum (Figs. 2B and 2C).

Three years later, the second ablation session was performed due to a relapse of persistent AF. This time, we identified 2 other PAC foci in the right atrium (Fig.

Table 1 Clinical Characteristics of Affected Individuals

Individual	Gender	Age (yrs)	Arrhythmias	Onset of PAC (yrs)	Onset of AF (yrs)	Mutation Carrier	HR (beats/min)	QRS (ms)	QTc	LAD (mm)	LVEF (%)	Antiarrhythmic Agents Used to Treat AF
I-2	F	90*	Unknown	NA	NA	ND	NA	NA	NA	NA	NA	NA
II-2	F	75*	Permanent AF	NA	NA	ND	88	74	427	36	79	—
II-3	F	75*	Paroxysmal AF, PACs	NA	NA	ND	77†	104†	478†	30	75	Disopyramide
III-1	M	60	Paroxysmal AF, PACs	NA	48	Yes	70	92	394	32	75	Disopyramide, cibenzoline, aprindine
III-3	M	57	Permanent AF	15	51	Yes	71	82	385	NA	NA	—
IV-1	M	34	PACs	23	—	Yes	68	82	399	ND	ND	—
IV-3	M	31	Persistent AF	18	27	Yes	65	81	388	30	63	Pilsicainide, flecainide
IV-4	F	29	Permanent AF	12	26	Yes	88	87	429	31	61	Pilsicainide

*Age of death; †disopyramide administration.
AF = atrial fibrillation; HR = heart rate; LAD = left atrial dimension; LVEF = left ventricular ejection fraction; NA = records not available; ND = not determined; PAC = premature atrial contraction.

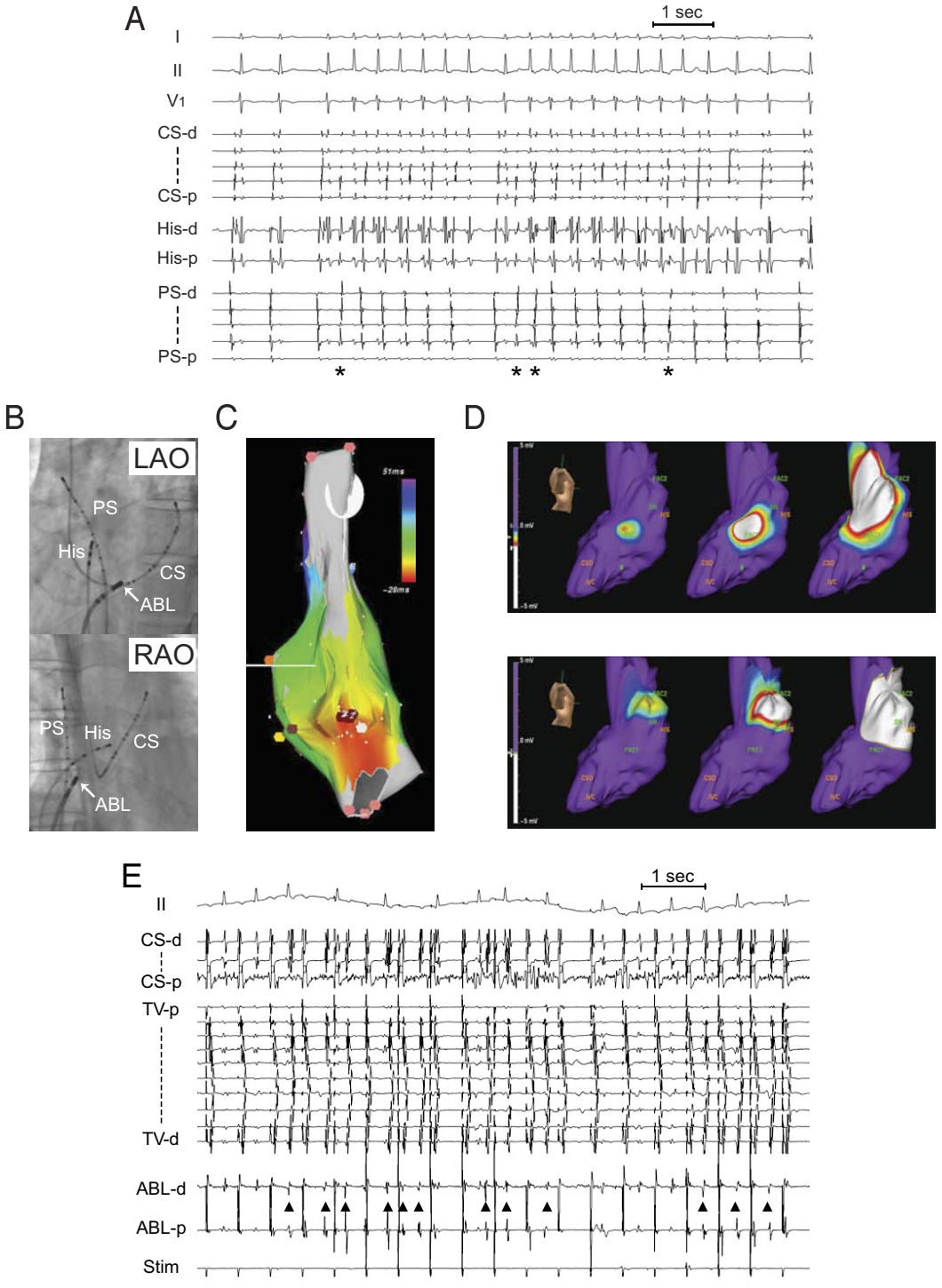

Figure 2 **Radiofrequency Catheter Ablation Recordings**

The first **(A to C)** and the second **(D and E)** ablation sessions on the proband. **(A)** Repetitive atrial tachycardias (ATs) from multiple origins. Shown are intracardiac recordings from the coronary sinus (CS), the His bundle (His), and a catheter placed along the posterior septum (PS) in the right atrium. Note that atrial activation sequences in CS during ATs were consistently proximal to distal, suggesting right atrial origins. **Asterisks** indicate the successfully ablated AT originating from the lower-right atrial septum. **(B)** Fluoroscopic images of the electrodes in the left anterior oblique (LAO) and right anterior oblique (RAO) views. Position of the ablation catheter (ABL; indicated by **arrows**); successful ablation site of the AT. **(C)** Three-dimensional electroanatomic map of the AT in the right posterior oblique view. The AT focus in the lower-right atrial septum was successfully ablated in the first session. **(D)** Noncontact mapping of PACs in the right lateral view. Two PAC foci in the middle of the crista terminalis **(upper panel)** and the high posterolateral wall **(lower panel)** ablated successfully in the second session are shown. **(E)** Numerous electrical firings (▲) from the contact site during radiofrequency energy delivery in generating tricuspid valve isthmus block. Continuous pacing was performed from proximal CS. Stim = stimulator; TV = tricuspid valve annulus; other abbreviations as in Figure 1.

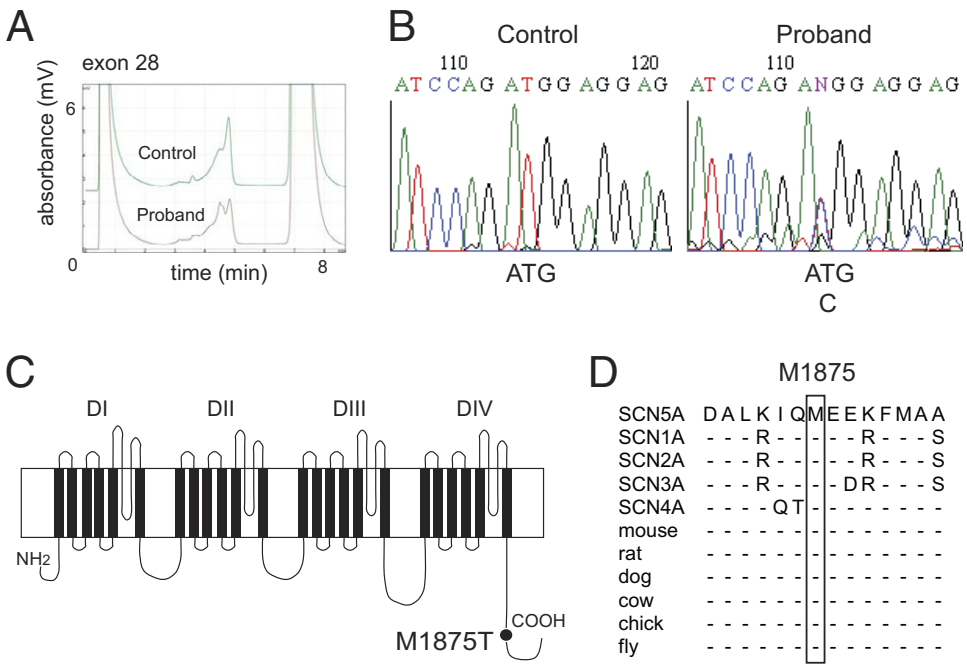

Figure 3 **Genetic Analysis**

(A) The denaturing high-performance liquid chromatography elution profiles for an *SCN5A* mutation, M1875T, detected in the affected family members. **(B)** Deoxyribonucleic acid sequencing electropherograms demonstrate heterozygosity for a *SCN5A* mutation. **(C)** Topology of the α-subunit of voltage-gated cardiac sodium (Na^+) channel. The location of the detected mutation is shown. **(D)** Amino acid sequence alignments of *SCN5A* with related Na^+ channels. The *SCN5A* indicates human heart; *SCN1A*, human brain type I; *SCN2A*, human brain type II; *SCN3A*, human brain type III; *SCN4A*, human skeletal muscle. The sequences of other species represent the cardiac isoforms of Na^+ channels.

2D)—both were successfully ablated. During the subsequent procedure to generate a cavotricuspid isthmus block, we noticed that energy delivery from the catheter induced numerous electrical firings from the contact sites (Fig. 2E). After the second ablation session, he maintained a sinus rhythm under medication, yet even after which he experienced occasional episodes of paroxysmal AF. Interestingly, after each attempt of cardioversion, ATs that lasted for several seconds were observed immediately after the shock was delivered and before sinus rhythm conversion (data not shown). All of these features strongly suggest the proband's increased vulnerability to atrial arrhythmias.

Genetic analysis. We identified a novel missense mutation, c.5624T>C, p.M1875T, in the *SCN5A* gene in the proband. Figure 3 shows the denaturing high-performance liquid chromatography and sequence results (Figs. 3A and 3B) and an illustration showing the position of the identified mutation (Fig. 3C). The amino acid at codon 1875 (methionine) is highly conserved among different Na^+ channel isoforms and species (Fig. 3D). Furthermore, this mutation was absent in 210 Japanese control individuals (420 chromosomes). We failed to identify mutations in any other potential candidate genes of familial AF (*KCNQ1*, *KCNH2*, *KCNE1*, *KCNE2*, *KCNE3*, *KCNJ2*, and *KCNA5*). Further analysis of the family members revealed that the M1875T mutation in SCN5A perfectly matched their clinical phenotypes (Figs. 1A and 1D, Table 1).

Functional analysis of M1875T-*SCN5A*. We performed biophysical assays for the novel *SCN5A* mutation with a heterologous expression system in HEK293 cells. Figure 4A illustrates representative whole-cell current traces from cells expressing wild-type (WT) and M1875T Na^+ channels in the presence of the coexpressed Na^+ channel β subunit.

Notably, M1875T channels showed an apparently slower inactivation compared with WT. The time constants for both fast and slow inactivation across a wide range of test potentials were significantly larger with M1875T in comparison with WT (Fig. 4B), indicating impaired inactivation. Figure 4C shows the peak current-voltage relation for WT and M1875T channels. The maximum current density of WT was observed at −20 mV but shifted to −30 mV for M1875T. In addition, the peak current density of M1875T was significantly larger than WT (WT, 326.2 ± 28.2 pA/pF, n = 23; M1875T, 484.6 ± 49.6 pA/pF, n = 31, $p < 0.01$) (Fig. 4D). As in WT, M1875T channels showed no persistent inward Na^+ currents at the end of a 200-ms depolarization (Fig. 4E), which is one of the defining mechanisms of QT interval prolongation in patients with LQTS3. The subtracted amplitude at the end of the 200-ms depolarization was 0.046 ± 0.009% (n = 5) of the peak current for WT and 0.048 ± 0.038% (n = 7) for M1875T.

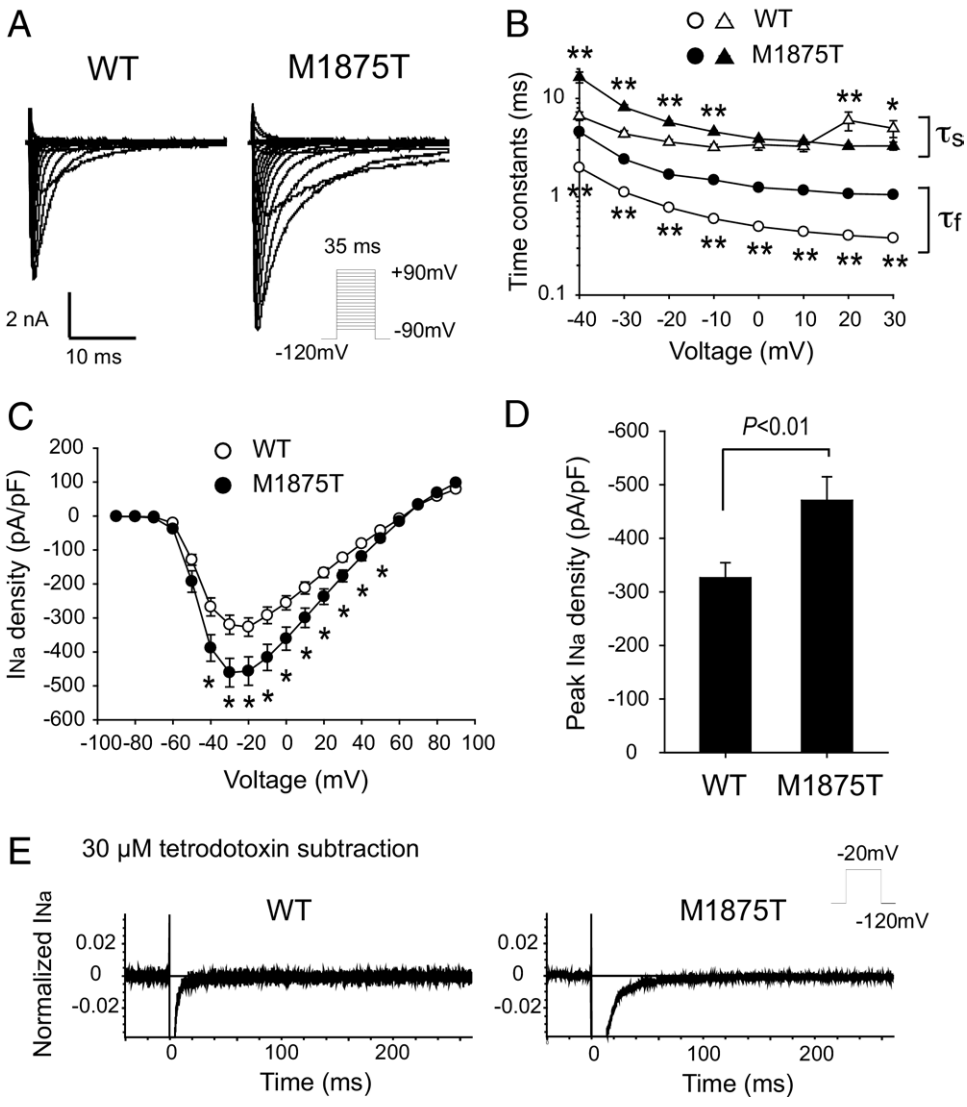

Figure 4 **Macroscopic Na^+ Currents of M1875T Channels**

(A) Representative whole-cell current traces of wild-type (WT) and M1875T sodium (Na^+) channels. Cells were transfected with human β1-subunit (protocol shown as an inset). **(B)** Voltage dependence of inactivation time constants. The time course of inactivation was fit with a 2 exponential equation: $I/I_{max} = A_f \times \exp(-t/\tau_f) + A_s \times \exp(-t/\tau_s)$. Lower and upper bundles of symbols indicate fast (τ_f) and slow (τ_s) time constant values, respectively. Statistically significant differences are indicated (*$p < 0.05$, **$p < 0.01$). **(C)** Average current-voltage relationship for WT and M1875T channels. The current is normalized to cell capacitance to give a measure of Na^+ current density. **Asterisks** indicate the voltages at which the current density was statistically different (*$p < 0.05$). **(D)** Average peak Na^+ current density of WT and M1875T channels. The peak current density was significantly larger in M1875T (WT at −20 mV, 326.2 ± 28.2 pA/pF, n = 23; M1875T at −30 mV, 484.6 ± 49.6 pA/pF, n = 31, $p < 0.05$). **(E)** Representative Na^+ current traces recorded in the absence or presence of 30 μmol/l tetrodotoxin. Tetrodotoxin-sensitive persistent currents were calculated by digital subtraction. M1875T channels showed no persistent inward Na^+ currents.

Figure 5A shows the conductance-voltage and steady-state inactivation curves for WT and M1875T channels. Numerical data pertaining to the biophysical properties therein are summarized in Table 2. The parameters for the activation gate were similar between WT and M1875T. In contrast, the half-maximal potential ($V_{1/2}$) for the steady-state inactivation of M1875T showed a marked positive shift (+16.4 mV) compared with that of WT (WT, $V_{1/2}$ = −78.08 ± 0.94 mV, n = 22; M1875T, $V_{1/2}$ = −61.68 ± 0.76 mV, n = 33, $p < 0.01$). The slope factor (k) for M1875T was significantly larger than that of WT (WT, k = −7.13 ± 0.12, n = 22; M1875T, k = −6.07 ± 0.16, n = 33, $p < 0.01$). The pronounced depolarizing shift of the inactivation gate is likely to increase Na^+ channel availability during excitation.

We also investigated the other kinetic properties of Na^+ channels: recovery from inactivation, onset of slow inactivation, and closed-state inactivation. Parameters of recovery from inactivation and onset of slow inactivation were identical between WT and M1875T (Figs. 5B and 5C,

JACC Vol. 52, No. 16, 2008
October 14, 2008:1326–34

Table 2 Biophysical Properties of WT and M1875T Channels

	WT	M1875T
Activation (mV)	(n = 23)	(n = 37)
$V_{1/2}$	−43.61 ± 0.79	−44.09 ± 0.72
k	6.53 ± 0.16	5.98 ± 0.18
Steady-state inactivation (mV)	(n = 22)	(n = 33)
$V_{1/2}$	−78.08 ± 0.94	−61.68 ± 0.76†
k	−7.13 ± 0.12	−6.07 ± 0.16†
Recovery from inactivation	(n = 16)	(n = 25)
A_f	0.84 ± 0.01	0.84 ± 0.01
A_s	0.15 ± 0.01	0.15 ± 0.01
τ_f (ms)	8.95 ± 0.95	8.32 ± 0.83
τ_s (ms)	338.6 ± 30.4	271.6 ± 31.6
Onset of slow inactivation	(n = 15)	(n = 16)
A	0.12 ± 0.01	0.12 ± 0.01
τ (ms)	773.9 ± 90.0	647.2 ± 70.6
Closed-state inactivation	(n = 9)	(n = 9)
A	0.13 ± 0.03	0.05 ± 0.02*
τ (ms)	97.1 ± 7.8	212.7 ± 22.3†

Data are mean ± SEM. Parameters were obtained from fitting individual experiments illustrated in Figure 4. *$p < 0.05$; †$p < 0.01$ versus wild-type (WT).

A and τ = fractional amplitude and time constant, respectively; n = number of tested cells; $V_{1/2}$ and k = midpoint potential and slope factor, respectively.

Table 2). With regard to closed-state inactivation, the extent was significantly less (WT, A = 0.13 ± 0.03 ms, n = 9; M1875T, A = 0.05 ± 0.02 ms, n = 9, $p < 0.05$), and the time constant was larger in the M1875T channels when compared with WT (WT, τ = 97.1 ± 7.8 ms, n = 9; M1875T, τ = 212.7 ± 22.3 ms, n = 9, $p < 0.01$) (Fig. 5D, Table 2). These data suggest that the number of inactivated M1875T channels is reduced near the resting potential.

Collectively, the M1875T mutation exhibited a gain-of-function type modulation in the cardiac Na^+ channels without persistent inward Na^+ currents: increased peak Na^+ channel density; prolonged time constants of both fast and slow inactivation; a large depolarizing shift in $V_{1/2}$ of the steady-state inactivation; and a lesser extent and a larger time constant with regard to closed-state inactivation. In short, the M1875T mutation clearly demonstrates characteristics that make it distinct from the LQTS3-type gain-of-function modulation.

Discussion

In the present study, we identified a novel gain-of-function *SCN5A* mutation that causes a familial form of AF. The clinical course of AF development materialized in a similar fashion among all affected family members (i.e., palpitations due to frequent PACs and ATs in their teens, followed by paroxysmal and then persistent AF). During the clinical electrophysiological study in the proband, we recognized multifocal activity sites and increased excitability in the right atrium. These distinguishing features are presumably associated with the unique biophysical properties of the mutant Na^+ channels. It should be noted, however, that the size of the pedigree analyzed in this study is limited.

***SCN5A* mutations and familial AF.** Mutations in *SCN5A* have been reported to cause a wide variety of cardiac arrhythmias. The gain-of-function mutations result in LQTS3 (5), whereas the loss-of-function mutations result in various phenotypes: 1) Brugada syndrome; 2) idiopathic ventricular fibrillation; 3) cardiac conduction disease; and 4) congenital sick sinus syndrome. We previously reported that *SCN5A*-linked Brugada syndrome is a high-risk group of bradyarrhythmias, linked predominantly to sick sinus syndrome (6). Although AF is a common complication of Brugada syndrome (10% to 30%) (6,15), there is a scarcity of reports on *SCN5A*-positive Brugada syndrome and AF.

Atrial fibrillation is the most common form of cardiac arrhythmia, characterized by rapid irregular activation of the atrium, and a common cause of morbidity and mortality. Atrial fibrillation occurs predominantly in elderly persons and is frequently associated with underlying cardiac diseases. In 15% to 30% of patients, however, an etiology is absent (i.e., lone AF) (16,17). Although AF has been regarded a sporadic and acquired disease, the familial aggregation of AF has been shown to be more frequent than previously recognized (18,19). Chen et al. (7) found the first gene mutation responsible for familial AF in *KCNQ1*, which encodes the α-subunit of slow delayed rectifier potassium (K^+) channels. Since then, 3 additional genes—all of which encode cardiac K^+ channels—responsible for familial AF have been identified: *KCNE2* (8), *KCNJ2* (9), and *KCNA5* (10). Recently, loss-of-function *SCN5A* mutations (D1275N) were reported to be associated with 2 families who have atrial arrhythmias (AF, cardiac conduction disease, and sick sinus syndrome) with dilated cardiomyopathy (11,12). More recently, an *SCN5A* mutation (N1986K) was identified in a family with lone AF (13). Functional assays on the N1986K channels revealed a hyperpolarized shift of steady-state inactivation, indicating a loss-of-function type modulation. One of the affected members underwent pacemaker implantation due to sick sinus syndrome, suggesting the underlying conduction disturbance resulting from the Na^+ channel loss-of-function. In addition, a common polymorphism (H558R) in *SCN5A*, present in 20% of the population (20), reduces Na^+ current density (21). The screening for the polymorphism in 157 patients with lone AF revealed that the R558 allele was more common in patients with lone AF than in the control subjects and as such was considered to be a risk factor for lone AF (22). However, none of the M1875T-positive individuals carried the R558 allele.

These reports implicate a potential relationship between decreased Na^+ currents and AF; however, to date, an *SCN5A* gain-of-function mutation has never been linked to AF.

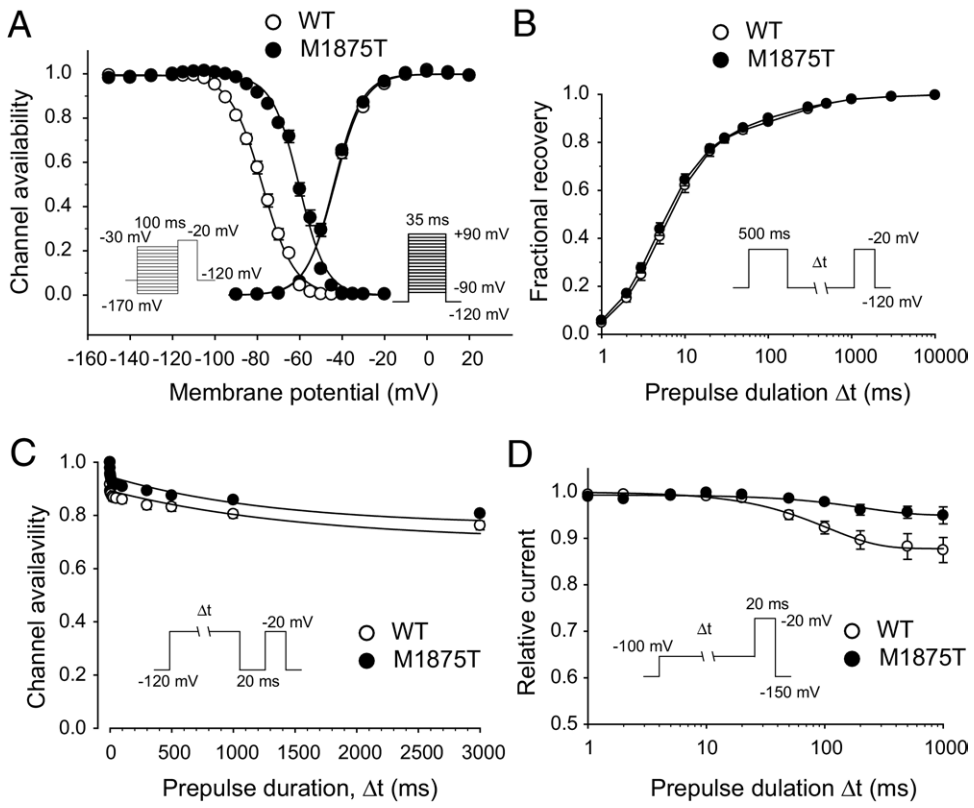

Figure 5 **Gating Properties for M1875T Channels**

Detailed parameters are given in Table 2. **(A)** Voltage dependence of relative sodium (Na^+) conductance activation and steady-state inactivation were determined by means of the voltage protocols, as shown in the inset. Curves were fit with the Boltzmann equation, $I/I_{max} = (1 + \exp[V-V_{1/2}]/k)^{-1}$ to determine the membrane potential for half-maximal inactivation or activation ($V_{1/2}$) and the slope factor *k*. Note that M1875T channels showed a pronounced depolarized shift (+16.4 mV) in the $V_{1/2}$ of steady-state inactivation compared with wild-type (WT). **(B)** Time course of recovery from inactivation was elicited with a double pulse protocol. Data were fit with a 2 exponential equation: $I/I_{max} = A_f \times (1 - \exp[-t/\tau_f]) + A_s \times (1 - \exp[-t/\tau_s])$, where A_f and A_s are fractions of fast and slow inactivation components, and τ_f and τ_s are the time constants of fast and slow inactivation components, respectively. **(C)** Onset of slow inactivation. Time course of entry into the slow inactivation state was obtained by a double pulse protocol. Curves were fit with a single exponential equation: $I/I_{max} = y0 + A \times \exp(-t/\tau)$. **(D)** Closed-state inactivation. The transfer rate of Na^+ channels from closed-state to inactivated closed-state without an intervening opening state was measured by a double pulse protocol. Time course for development of closed-state inactivation was fit with a single exponential equation: $I/I_{max} = y0 + A \times \exp(-t/\tau)$. The extent of closed-state inactivation was significantly less and the time constant larger in M1875T channels in comparison with WT.

Unique gain-of-function properties of M1875T Na^+ channels. To date, *SCN5A* gain-of-function mutations have been reportedly linked to only 1 phenotype, LQTS3. Persistent inward Na^+ currents observed in these mutant channels are considered to cause QT prolongation. However, M1875T channels did not display persistent inward Na^+ currents (Fig. 4E). This might explain why all of the affected and mutation-positive individuals in our study exhibited normal QT interval, with the exception of 1 individual who received disopyramide therapy. The functional properties of M1875T Na^+ channels were quite distinct from those of LQTS3. The most prominent change was a +16.4 mV shift in the steady-state inactivation. This is, to the best of our knowledge, the greatest depolarization shift in all of the previously reported SCN5A mutants. Some of the LQTS3 mutants (E1295K, A1330P, A1330T, and I1768V) showed a similar depolarizing shift of the steady-state inactivation without persistent inward Na^+ currents; however, the extent of the depolarizing shift was much less than M1875T (all were <+10 mV). The M1875T channels displayed the increased peak Na^+ current density (Fig. 4D), perhaps due to the large depolarized shift in steady-state inactivation. Interestingly, the location of the mutation is within a complex region that includes Ca^{2+} binding EF-hand like motifs and a putative binding site for calmodulin (23), and thus the mutation might disrupt inactivation by altered calcium sensitivity.

The potential mechanisms by which the identified gain-of-function mutation might lead to PAC or AF could be explained as the following: first, increased inward Na^+ currents might cause repolarization failure or early afterdepolarizations, thereby inducing triggered activities; and second, the increased Na^+ currents might increase the conduction velocity and facilitate the maintenance of the fibrillation wave. However, further studies are needed to elucidate the underlying mechanisms.

Genotype–phenotype relationship and clinical implications. Quite impressively, the affected family members shared a similar clinical course with high penetrance—frequent PACs and ATs first appeared during their teens and subsequently progressed to AF (Fig. 1A). Increased automaticity and irritability in the atrium was demonstrated by recurrent atrial arrhythmias that were resistant to ablation or drug therapy, induced PACs during exercise (Fig. 1C), and numerous ectopic firings and increased excitability throughout the right atrium during catheter ablation (Fig. 2). Because Na^+ channels encoded by *SCN5A* are expressed in both the atrium and ventricle, it remains unknown why our patients showed only atrial arrhythmias but not ventricular arrhythmias. The different electrophysiological properties between atrial and ventricular cells might be the underlying cause. Resting membrane potential is more depolarized, and the peak Na^+ current density is larger in atrial cells than in ventricular cells in dogs (24). The critical depolarization and current threshold for action potential initiation are smaller in atrial cells than in ventricular cells, indicating that atrial cells are more readily excitable than ventricular cells (25).

Conclusions

We identified a novel *SCN5A* gain-of-function mutation that causes a familial form of AF without any underlying structural heart diseases, which provides us with new insight into the pathogenesis of the commonly occurring form of AF.

Acknowledgment

The authors thank Richard Kaszynski for his critical reading of the manuscript.

Reprint requests and correspondence: Dr. Masaharu Akao, Department of Cardiovascular Medicine, Kyoto University Graduate School of Medicine, 54 Shogoin Kawahara-cho, Sakyo-ku, Kyoto, 606-8507, Japan. E-mail: akao@kuhp.kyoto-u.ac.jp.

REFERENCES

1. Chen Q, Kirsch GE, Zhang D, et al. Genetic basis and molecular mechanism for idiopathic ventricular fibrillation. Nature 1998;392:293–6.
2. Akai J, Makita N, Sakurada H, et al. A novel SCN5A mutation associated with idiopathic ventricular fibrillation without typical ECG findings of Brugada syndrome. FEBS Lett 2000;479:29–34.
3. Schott JJ, Alshinawi C, Kyndt F, et al. Cardiac conduction defects associate with mutations in SCN5A. Nat Genet 1999;23:20–1.
4. Benson DW, Wang DW, Dyment M, et al. Congenital sick sinus syndrome caused by recessive mutations in the cardiac sodium channel gene (SCN5A). J Clin Invest 2003;112:1019–28.
5. Wang Q, Shen J, Splawski I, et al. SCN5A mutations associated with an inherited cardiac arrhythmia, long QT syndrome. Cell 1995;80:805–11.
6. Makiyama T, Akao M, Tsuji K, et al. High risk for bradyarrhythmic complications in patients with Brugada syndrome caused by SCN5A gene mutations. J Am Coll Cardiol 2005;46:2100–6.
7. Chen YH, Xu SJ, Bendahhou S, et al. KCNQ1 gain-of-function mutation in familial atrial fibrillation. Science 2003;299:251–4.
8. Yang Y, Xia M, Jin Q, et al. Identification of a KCNE2 gain-of-function mutation in patients with familial atrial fibrillation. Am J Hum Genet 2004;75:899–905.
9. Xia M, Jin Q, Bendahhou S, et al. A Kir2.1 gain-of-function mutation underlies familial atrial fibrillation. Biochem Biophys Res Commun 2005;332:1012–9.
10. Olson TM, Alekseev AE, Liu XK, et al. Kv1.5 channelopathy due to KCNA5 loss-of-function mutation causes human atrial fibrillation. Hum Mol Genet 2006;15:2185–91.
11. McNair WP, Ku L, Taylor MRG, et al. SCN5A mutation associated with dilated cardiomyopathy, conduction disorder, and arrhythmia. Circulation 2004;110:2163–7.
12. Olson TM, Michels VV, Ballew JD, et al. Sodium channel mutations and susceptibility to heart failure and atrial fibrillation. JAMA 2005;293:447–54.
13. Ellinor PT, Nam EG, Shea MA, Milan DJ, Ruskin JN, Macrae CA. Cardiac sodium channel mutation in atrial fibrillation. Heart Rhythm 2008;5:99–105.
14. Shirai N, Makita N, Sasaki K, et al. A mutant cardiac sodium channel with multiple biophysical defects associated with overlapping clinical features of Brugada syndrome and cardiac conduction disease. Cardiovasc Res 2002;53:348–54.
15. Bordachar P, Reuter S, Garrigue S, et al. Incidence, clinical implications and prognosis of atrial arrhythmias in brugada syndrome. Eur Heart J 2004;25:879–84.
16. Murgatroyd FD, Camm AJ. Atrial arrhythmias. Lancet 1993;341:1317–22.
17. Levy S, Maarek M, Coumel P, et al. Characterization of different subsets of atrial fibrillation in general practice in France: the ALFA study. Circulation 1999;99:3028–35.
18. Darbar D, Herron KJ, Ballew JD, et al. Familial atrial fibrillation is a genetically heterogeneous disorder. J Am Coll Cardiol 2003;41:2185–92.
19. Ellinor PT, Yoerger DM, Ruskin JN, MacRae CA. Familial aggregation in lone atrial fibrillation. Hum Genet 2005;118:179–84.
20. Ackerman MJ, Splawski I, Makielski JC, et al. Spectrum and prevalence of cardiac sodium channel variants among black, white, Asian, and Hispanic individuals: implications for arrhythmogenic susceptibility and Brugada/long QT syndrome genetic testing. Heart Rhythm 2004;1:600–7.
21. Makielski JC, Ye B, Valdivia CR, et al. A ubiquitous splice variant and a common polymorphism affect heterologous expression of recombinant human SCN5A heart sodium channels. Circ Res 2003;93:821–8.
22. Chen LY, Ballew JD, Herron KJ, Rodeheffer RJ, Olson TM. A common polymorphism in SCN5A is associated with lone atrial fibrillation. Clin Pharmacol Ther 2007;81:35–41.
23. Deschenes I, Neyroud N, DiSilvestre D, Marban E, Yue DT, Tomaselli GF. Isoform-specific modulation of voltage-gated Na(+) channels by calmodulin. Circ Res 2002;90:E49–57.
24. Burashnikov A, Di Diego JM, Zygmunt AC, Belardinelli L, Antzelevitch C. Atrium-selective sodium channel block as a strategy for suppression of atrial fibrillation: differences in sodium channel inactivation between atria and ventricles and the role of ranolazine. Circulation 2007;116:1449–57.
25. Golod DA, Kumar R, Joyner RW. Determinants of action potential initiation in isolated rabbit atrial and ventricular myocytes. Am J Physiol Heart Circ Physiol 1998;274:H1902–13.

Key Words: arrhythmia ■ atrial fibrillation ■ genetics ■ ion channels ■ sodium.